植物としてのトキソプラズマ原虫

植物ホルモンとカルシウムシグナリング

Toxoplasma gondii as a plant：Plant hormone and calcium signaling

永宗喜三郎

トキソプラズマ原虫は，植物ホルモンの一種であるアブシジン酸を使って互いに「コミュニケーション」を行い，宿主細胞内で増殖した後の脱出のタイミングを決めていた．アブシジン酸濃度の上昇は，原虫細胞質内カルシウム濃度の上昇をひき起こし，その結果，宿主からの脱出のためのさまざまなイベントが開始されていた．アブシジン酸生合成を阻害すると，原虫はシストへと分化していくことも示された．トキソプラズマ原虫においてこの植物ホルモン産生能は，紅藻が原虫内に共生することにより獲得された細胞内小器官に由来するものと思われた．

Key words ● トキソプラズマ原虫 ● アブシジン酸 ● アピコプラスト ● 色素体 ● 進化

はじめに

トキソプラズマ原虫はほとんどの温血動物のすべての有核細胞に感染能をもち，全人類の1/3以上，日本人の約25～30％が感染しているといわれている非常に広く蔓延している寄生性原生生物である[1]．多くの感染者にとって，トキソプラズマ感染は不顕性に経過するが，一方でトキソプラズマ感染症は一度発症すると非常に重篤な感染症となる．1999年CDC（米国疾病予防管理センター）からの報告の中では，トキソプラズマ症は，食品由来の感染症による全入院患者のうち原因の明らかになったものの4.1％（第4位），死者数においては20.7％（第3位）にもなると推定されている[2]．また，トキソプラズマ原虫はHIV感染者に致死的な脳炎をひき起こして患者を死に至らしめることが知られており，アメリカでの統計によるとHIV感染患者の18～25％がトキソプラズマ脳炎を発症することが報告されている[3]．一方1999年WHOからの報告によると[4]，1998年の全世界の総死者数の25％を占める感染症による死者のうち，17.3％がAIDSを原因として亡くなっていることと合わせて考えると，世界中の感染症による死者の約4％はトキソプラズマ感染症が原因で亡くなっていると見積もることができる．

トキソプラズマ原虫がヒトに感染した場合，その増殖はタキゾイトとブラディゾイトという2つのステージに分けることができる（図1）．タキゾイトは宿主細胞内に形成された小胞内で急速に増殖するステージで，宿主細胞内への侵入，分裂，宿主細胞からの脱出と次の宿主細胞への移動と付着を次々と繰り返し，感染を広げていく．一方，ブラディゾイト，あるいはシストとよばれるステージでの原虫の分裂は非常に緩慢で，おもに中枢神経系や筋肉系に存在している．シストとなった原虫は宿主の免疫応答から逃れ，宿主が免疫抑制状態になり再活性化できるまで長期間生存する．再活性化した原虫はふたたびタキゾイトとなり感染を再拡大し，宿主の組織を破壊する．

トキソプラズマ原虫が属する，アピコンプレクス門に属する原虫には現在5,000種以上が知られており，すべてが寄生性の原生動物である[5]．このなかにはマラリア原虫やトキソプラズマ原虫，クリプトスポリジウム原虫など人類にとって大きな脅威となっている感染症が含まれている[2,4]．これらアピコンプレクス門に属する原虫の大きな特徴の一つとして，アピコプラストとよばれるオルガネラの存在が挙げられる．アピコプラストは葉緑体が退化してできた四重膜構造の細胞内小器官であり，通常の葉緑体は光合成細菌が植物の祖先に取り込まれて進化したものとされているが，アピコプラストは光合成細菌を取り込んだ紅藻類の祖先が原虫の祖先生物に取り込まれることによって成立したと考えられている[6]（図2）．その

Kisaburo Nagamune
筑波大学大学院・生命環境科学研究科・若手イニシアティブ，現 国立感染症研究所寄生動物部
E-mail：nagamune@nih.go.jp
URL：http://web.me.com/nagamune

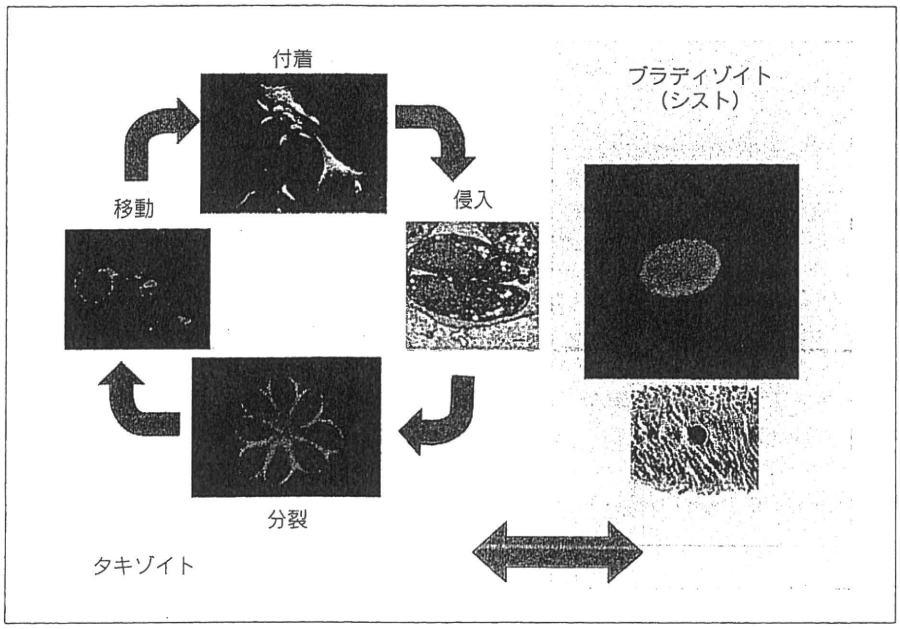

図1　トキソプラズマ原虫の増殖サイクル

ヒトに感染したトキソプラズマ原虫は活発な増殖ステージであるタキゾイトか，あるいは緩慢な増殖ステージであるブラディゾイト(シスト)かのいずれかのかたちで寄生している．タキゾイトのステージにある原虫は，宿主細胞への付着，侵入，宿主細胞内での分裂，宿主細胞を破壊して脱出，次の細胞への移動，というサイクルを繰り返し，活発に増殖を続ける．一方で，ブラディゾイトのステージにある原虫は増殖がほとんど停止し，宿主からの免疫応答から逃れるため被嚢し，再活性化の機会を待つ．

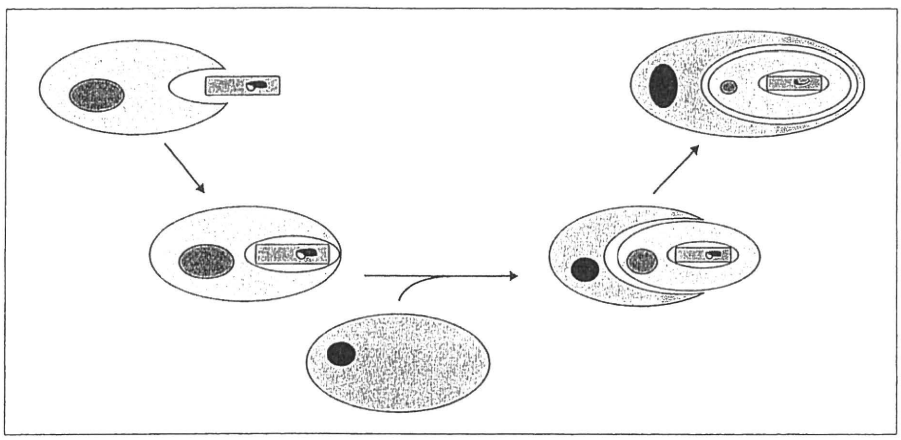

図2　アピコプラストの成立機序

通常の葉緑体は光合成細菌（緑）が植物の祖先（青）に取り込まれて進化したものとされているが，アピコプラストは光合成細菌を取り込んだ紅藻類の祖先が原虫の祖先生物（赤）に取り込まれることによって成立したと考えられている．そのために，アピコプラストは独特の四重膜構造をとる．

ために，アピコプラストは独特の四重膜構造をとる．現在ではアピコプラストは光合成能を失ったものの，脂肪酸合成などの機能を今でも担っており，したがって原虫にとって必須のオルガネラである[7]．しかしながらその機能の詳細は不明であり，なぜ原虫の生存に必須なのかもはっきりとはわかっていない．いずれにしても，アピコンプレクス門原虫の細胞内には植物が「組み込まれている」ということは今やよく知られた事実となっている．最近，筆者らは，トキソプラズマ原虫が植物ホルモンの一種であるアブシジン酸を産生しており，それがトキソプラズマ原虫の細胞質内カルシウム濃度調節をつかさどっていることを明らかにした[8]．本稿では，トキソプラズマ原虫における細胞質内カルシウム濃度調節機構と，植物ホルモンであるアブシジン酸の原虫における意義について考察したい．

I トキソプラズマ原虫の運動・分泌とカルシウムシグナリング

トキソプラズマ原虫は，鞭毛や繊毛のような移動のための特別な器官をもたない．そのため原虫の宿主細胞への侵入は，いわゆる「グライディング」とよばれる原虫アクチン依存的な運動により行われていることが知られている[9]．その際，原虫はマイクロネームとよばれる分泌器官から多数の付着分子を分泌することにより，宿主細胞への付着・侵入が可能となる．このマイクロネーム蛋白質が分泌されるには，原虫の細胞質内カルシウム濃度の上昇が必要である[10]．また，原虫が宿主細胞から脱出す

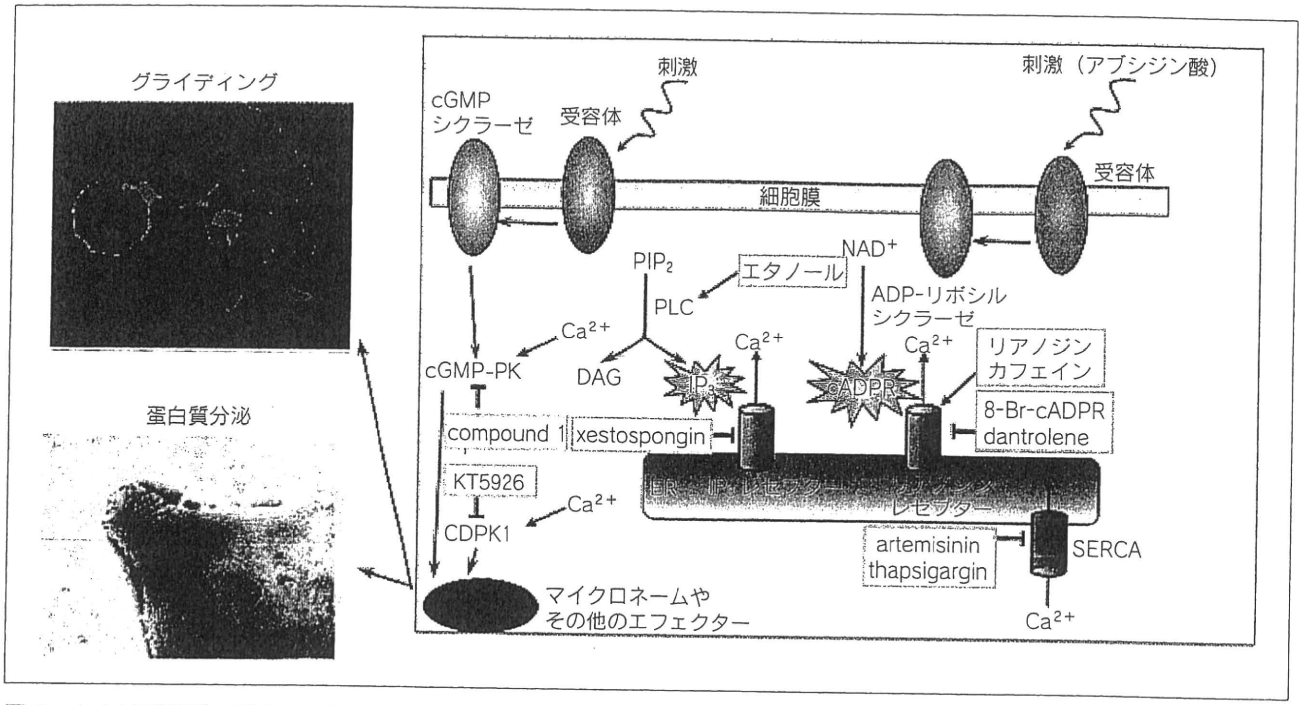

図 3　トキソプラズマ原虫のカルシウムシグナル伝達機構

トキソプラズマ原虫細胞質内カルシウム濃度の上昇は原虫のマイクロネームからの蛋白質分泌や原虫のグライディングを活性化する[13,24,25]．細胞内カルシウム・プールからのカルシウム放出には，cADPR 産生依存的な経路[13]と，IP_3 産生依存的な経路の 2 つがあることが知られている[26]．前者の経路はリアノジンやカフェインにより活性化し，8-Br-cADPR や dantrolene により阻害され，後者の経路はエタノールにより活性化し，xestospongin によって阻害される．カルシウムの再取込みは SERCA によって行われ，thapsigargin や抗マラリア薬である artemisinin は SERCA による細胞質内カルシウムの取込みを阻害していると考えられている[27,28]．細胞質内カルシウム濃度が上昇した後，calcium-dependent protein kinase 1(CDPK1)および cGMP-dependent protein kinase(cGMP-PK)の 2 種類のキナーゼがマイクロネーム蛋白質の分泌に必要であることが報告されている[29,30]．これらのキナーゼはそれぞれ KT5926 および compound 1 により阻害される．これら一連のシグナルを活性化する刺激としては，アブシジン酸が cADPR 依存的なカルシウム放出経路を活性化することが明らかとなった．アブシジン酸および他の刺激に対するレセプターはいまだ明らかになっていない．

るタイミングも細胞質内カルシウム濃度によって調節されることが知られている[11]．薬理学的な解析により，トキソプラズマ原虫は他の生物同様に IP_3 レセプターやリアノジンレセプターを細胞内カルシウム・プールからのカルシウム放出に用いていることが示されてきた．しかしながら，トキソプラズマ原虫に限らず，すべてのアピコンプレクス門原虫のゲノムデータベースからは，ヒトやマウスなどの動物で知られているこれらのレセプターのオルソログ遺伝子は見つからなかった．そこで筆者らはアピコンプレクス門に属する，トキソプラズマ，マラリア，およびクリプトスポリジウム原虫のゲノムデータベースから既知のすべてのカルシウム濃度調節分子遺伝子の同定を試みた[12]．その結果，これらの原虫のカルシウム濃度調節機構は多くの動物のものとは異なり，むしろ，植物的であることを明らかにできた．たとえば，アピコンプレクス門原虫は通常の IP_3 レセプター遺伝子をもっておらず，今まで植物のみで報告されている two-pore calcium

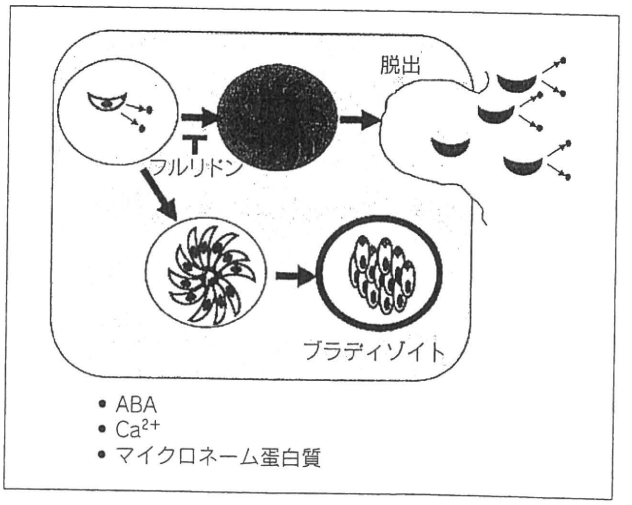

図 4　植物ホルモンであるアブシジン酸がトキソプラズマ原虫に及ぼす影響

アブシジン酸（ピンクの丸）の蓄積が原虫細胞質内カルシウム（青）濃度の上昇をひき起こし，原虫は宿主細胞からの脱出やマイクロネーム蛋白質（緑の丸）の分泌を開始する．フルリドンはアブシジン酸の生合成を阻害し，原虫の脱出を抑制してブラディゾイトへの分化を促進させる．

channel（TPC）遺伝子の存在が見出された．また，同様にこれらの原虫には，植物のみに認められ動物には存在しないとされる，calcium-dependent protein kinase（CDPK）遺伝子が多数認められた．

一方で，動物，植物ともにリアノジンレセプターを介した細胞質内へのカルシウム放出には，サイクリックADPリボース（cADPR）がセカンドメッセンジャーとして広く使われていることが知られている．トキソプラズマ原虫においても，筆者らは，cADPRがセカンドメッセンジャーとして細胞質内カルシウム濃度の上昇をひき起こすことを証明した[13]．また，筆者らは原虫のcADPR合成活性および分解活性を生化学的に証明し，cADPRのアンタゴニストである8-Br-cADPRやdantroleneはトキソプラズマ原虫において，マイクロネーム蛋白質の分泌および原虫のグライディングを阻害することを明らかにした．図3に筆者らや他のグループによって今までに明らかになったトキソプラズマ原虫のカルシウムシグナルの概略を示した．

植物においては，cADPRは植物ホルモンの一種であるアブシジン酸によって産生が誘導され，cADPR産生は植物においても細胞質内カルシウム濃度の上昇をひき起こすことが知られている．またアブシジン酸は，ヒドラや海綿においてもcADPR産生を介した細胞質内カルシウム濃度の上昇をひき起こすことが観察されている[14,15]．また最近，ヒト顆粒球においてもアブシジン酸によるcADPR依存的な細胞質内カルシウム濃度の上昇活性が報告された[16]．これらの事実は，アピコンプレクス門原虫においてもアブシジン酸依存的なcADPRを介したカルシウム放出経路が存在する可能性を示唆しうる．

II トキソプラズマ原虫におけるアブシジン酸

アブシジン酸をトキソプラズマ原虫に添加すると，前述のとおり原虫の運動や宿主細胞への侵入に重要な役割をもつマイクロネーム蛋白質の分泌が誘導された．また筆者らはすでに，マイクロネーム蛋白質の分泌はcADPR依存的な原虫細胞質内カルシウム濃度の上昇に依存していることを見出していたので，実際にアブシジン酸添加後に原虫の産生するcADPRを測定したところ，加えたアブシジン酸量に依存して有意に上昇していた．また，このアブシジン酸によるマイクロネーム蛋白質分泌は細胞質内カルシウム濃度の上昇に依存していることが確認できた．さらにこの活性は天然型のアブシジン酸にのみ存在し，その光学異性体やβ-カロテン，また，レチノイン酸には存在しなかった．

さらに筆者らはELISAやMS解析により，トキソプラズマ原虫が実際にアブシジン酸を産生していることを証明した．アブシジン酸濃度は原虫が宿主細胞から脱出する直前に急激に上昇していた．MS/MS解析により，トキソプラズマ原虫はトランス型およびシス型の両方のアブシジン酸を産生していることが示された．原虫の培養中にアブシジン酸は0.1～0.2μM（通常期）から～4μM（脱出直前）存在していた．これらの値はヒト顆粒球で報告された値の40倍にもなることから，原虫は環境中からアブシジン酸を取り込んでいるのではなく，自らが産生していると考えられる．宿主細胞内の原虫に，外部からアブシジン酸を加えると，原虫の宿主細胞からの脱出が誘導された．また，植物においてアブシジン酸生合成の特異的阻害剤であることが知られているフルリドンは，トキソプラズマ原虫においてもアブシジン酸産生を阻害した．そこで原虫の培養をフルリドン処理すると，トキソプラズマ原虫は加えたフルリドンの濃度依存的に宿主細胞からの脱出が阻害された．しかしながらこの阻害は外部からのアブシジン酸添加によって相補できた．これらのことからアブシジン酸は原虫にとって，宿主細胞からの脱出のシグナルになっている可能性が考えられた．以上の結果から，トキソプラズマ原虫はアブシジン酸を産生しており，アブシジン酸は原虫内でカルシウム放出のセカンドメッセンジャーであるcADPR産生を誘導し，細胞質内カルシウム濃度を上昇させ，宿主細胞からの脱出やそれに伴うグライディングと次の宿主細胞への侵入を促進するという一連のシグナルの存在が示唆された（図4）．

また，アブシジン酸生合成阻害剤フルリドンの培養中への添加によってアブシジン酸の生合成を阻害すると，原虫のブラディゾイトへの分化が誘導された（図1, 4）．高等植物において，アブシジン酸は種子の休眠状態を維持したり，発芽を抑制したりすることにより，発育を抑制的にコントロールしていることが知られている[17]．また高等植物においては，浸透圧，低温，塩などによるストレスによりアブシジン酸生合成遺伝子の発現レベルが上昇することも報告されている[17]．したがってアブシジン酸は植物にとって一種の「抗ストレスホルモン」として，

ストレス条件に対する耐性の上昇にはたらいていると考えることもできる．トキソプラズマ原虫においてはアブシジン酸の濃度の減少がブラディゾイトへの分化，すなわち休眠状態への移行を誘導したことから，植物で知られている抗ストレス反応とは，一見逆に見える作用を示した．トキソプラズマ原虫にとって通常，ブラディゾイトによる休眠は，栄養の不足や種々のストレスによってひき起こされるストレス応答の一種であると考えられている[18]ので，トキソプラズマ原虫においてもアブシジン酸が「抗ストレスホルモン」としてはたらいているのであれば，フルリドンによるアブシジン酸生合成の減少は，原虫を環境中のストレスへの耐性を減少させる方向にはたらき，それによって高濃度のアブシジン酸存在下で抑制されていた分化へのパスウエィが動き始めるのかもしれない．

フルリドンは一方で，マウスを用いたトキソプラズマ感染実験において，マウスの致死率を有意に減少させた．このことは，アブシジン酸生合成の阻害が原虫の宿主細胞からの脱出を抑制することによる感染拡散の阻止の結果であると推定できた．この結果はフルリドンが哺乳動物に対し毒性が弱く，除草剤として用いられている事実と合わせて考えると，フルリドン，あるいはアブシジン酸生合成阻害剤は抗トキソプラズマ薬開発のよいリード化合物となる可能性が示唆される．

おわりに

マラリアやトキソプラズマ原虫をはじめとする，多くのアピコンプレクス門原虫はアピコプラストとよばれる紅藻由来の共生器官をもっていることから，これらアピコンプレクス門原虫は葉緑体由来の多くの代謝経路をいまだ保持している可能性が考えられている．事実，アピコンプレクス門原虫はイソプレノイドを合成するための経路（メバロチン経路）を消失しており，そのためイソプレノイド合成は，アピコプラストに存在している植物と同じDOXP-MEP経路に依存していることが知られている[9]．高等植物において，アブシジン酸の生合成の多くは葉緑体内で行われていることと，アブシジン酸生合成はイソプレノイドからβ-カロテンを合成することにより開始されることから[19]，おそらくトキソプラズマ原虫においてもアブシジン酸生合成の大部分はアピコプラストにおいて行われている可能性が示唆できる．また，アピコンプレクス門原虫においてすでに光合成能を失ったアピコプラストがいまだ原虫の生存に必須であるという理由の一つに，今回見出されたアブシジン酸生合成経路の存在があるのかもしれない．

筆者らはアブシジン酸生合成遺伝子オルソログ候補遺伝子をトキソプラズマおよびマラリアゲノムデータベースからいくつか同定している．しかしながらこれらの遺伝子は高等植物の遺伝子とのホモロジーが低く，また，既知のすべての遺伝子が同定できたわけでもない．このことは，おそらく，原虫のアブシジン酸生合成経路がアピコプラスト由来，すなわち紅藻由来であるためであると思われる．高等植物においてもアブシジン酸生合成の大部分が葉緑体で行われていることから，アブシジン酸生合成経路が藍藻，あるいは真核藻類に保存されている可能性は低くないものと思われる．実際，緑藻，紅藻，褐藻，さらには原核生物である藍藻類にまでアブシジン酸産生能力があることが報告されている[20–23]．しかしながらこれら藻類のアブシジン酸生合成経路はあまりよくわかっていない．今後各藻類のアブシジン酸生合成経路および生合成にかかわる遺伝子群が明らかとなれば，トキソプラズマ原虫のアブシジン酸生合成経路の起源，つまりアピコンプレクス門原虫におけるアピコプラストの起源が明らかとなり，トキソプラズマ原虫やマラリア原虫の進化の過程を理解することに一つの大きなヒントを得ることができると考えられる．また，同時に効果的な抗原虫薬開発への大きな足がかりになる可能性が期待できる．

文　献

1) Dubey, J. P.：*in* "Toxoplasma gondii", (edited by Weiss, L. M., Kim, K.), pp. 1-17, Academic Press (2007)
2) Mead, P. S. *et al.*：*Emerging Infect. Dis.*, 5, 607-625 (1999)
3) Kasper, L. H., Buzoni-Gatel, D.：*Parasitol. Today*, 14, 150-156 (1998)
4) "World Health Organization Report on Infectious Diseases：Removing obstacles to healthy development", WHO (1999)
5) Levine, N. D.："The Protozoan Phylum Apicomplexa", CRC Press (1988)
6) Archibald, J. M., Keeling, P. J.：*Trends Genet.*, 18, 577-584 (2002)
7) Ralph, S. A. *et al.*：*Nat. Rev. Microbiol.*, 2, 203-216 (2004)
8) Nagamune, K. *et al.*：*Nature*, 451, 207-210 (2008)
9) Sibley, L. D.：*Science*, 304, 248-253 (2004)
10) Lovett, J. L., Sibley, L. D.：*J. Cell Sci.*, 116, 3009-3016 (2003)
11) Black, M. W. *et al.*：*Mol. Cell Biol.*, 20, 9399-9408 (2000)
12) Nagamune, K., Sibley, L. D.：*Mol. Biol. Evol.*, 23, 1613-1627

(2006)
13) Chini, E. N. *et al.* : *Biochem. J.*, 389, 269-277 (2005)
14) Puce, S. *et al.* : *J. Biol. Chem.*, 279, 39783-39788 (2004)
15) Zocchi, E. *et al.* : *Proc. Natl. Acad. Sci. USA*, 98, 14859-14864 (2001)
16) Bruzzone, S. *et al.* : *Proc. Natl. Acad. Sci. USA*, 104, 5759-5764 (2007)
17) Xiong, L., Zhu, J. K. : *Plant Physiol.*, 133, 29-36 (2003)
18) Weiss, L. M., Kim, K. : *in* "Toxoplasma gondii", (edited by Weiss, L. M., Kim, K.), pp. 341-366, Academic Press (2007)
19) Schwartz, S. H. *et al.* : *Plant Phyiol.*, 131, 1591-1601 (2003)
20) Hirsch, R. *et al.* : *Botanica Acta*, 102, 326-334 (1989)
21) Cowan, A. K., Rose, P. D. : *Plant Physiol.*, 97, 798-803 (1991)
22) Marsalek, B. *et al.* : *J. Plant Physiol.*, 139, 506-508 (1992)
23) Kobayashi, M. *et al.* : *Plant Growth Reg.*, 22, 79-85 (1997)
24) Carruthers V. B. *et al.* : *Biochem. J.*, 342, 379-386 (1999)
25) Carruthers V. B. *et al.* : *Cell Microbiol.*, 1, 225-235 (1999)
26) Lovett J. L. *et al.* : *J. Biol. Chem.*, 277, 25870-25876 (2002)
27) Nagamune, K. *et al.* : *Antimicrob. Agents Chemother.*, 51, 3816-3823 (2007)
28) Nagamune, K. *et al.* : *Eukaryotic Cell*, 6, 2147-2156 (2007)
29) Kieşchnick, H. *et al.* : *J. Biol. Chem.*, 276, 12369-12377 (2001)
30) Wiersma, H. I. *et al.* : *Int. J. Parasitol.*, 34, 369-380 (2004)

doi: 10.1111/j.1346-8138.2009.00592.00594.x

Journal of Dermatology 2009; **36**: 86–89

CASE REPORT

Case of creeping disease treated with ivermectin

Yuko SENBA,[1] Kenshiro TSUDA,[1] Haruhiko MARUYAMA,[2] Ichiro KUROKAWA,[3] Hitoshi MIZUTANI,[3] Yoshiki TANIGUCHI[1]

[1]*Department of Dermatology, Yokkaichi Municipal Hospital, Mie,* [2]*Division of Parasitology, Department of Infectious Diseases, Faculty of Medicine, University of Miyazaki, Kiyotake, Miyazaki, and* [3]*Department of Dermatology, Mie University Graduate School of Medicine, Mie, Japan*

ABSTRACT

We report a case of creeping disease treated successfully with ivermectin. A 46-year-old man presented with a 1-month history of pruriginous linear erythema on his right thigh after a visit to Indonesia. Although he had no history of eating raw fish or meat, he walked along the river and in the jungle without wearing shoes. Creeping disease caused by animal hookworm was strongly suspected. The presence of parasite larvae was not confirmed in biopsied skin specimens. In enzyme-linked immunosorbent assay, serum samples were negative for binding to hookworm antigens, including Ancylostoma canium, Necator americanus and Gnathostoma doloresi. He was treated with a single 12 mg oral dose (200 μg/kg) of ivermectin. The eruption and pruritus resolved within a few days after the administration and did not relapse.

Key words: ancylostoma, creeping eruption, hookworm, ivermectin, larva migrans.

INTRODUCTION

Creeping disease (cutaneous larva migrans) is a skin disease due to infection by the larval form of nematodes. In Japan, creeping disease caused by Gnathostoma spp. is most common in people who eat freshwater fish or the Japanese copperhead snake, whereas larval hookworm infection such as Ancylosotoma canium and Ancylostoma brasilliense is rare and is usually present as percutaneous infection.[1]

Ivermectin has been commonly used against onchocerciasis and scabies.[2] Recently, some cases have been reported of creeping disease treated successfully by oral administration of ivermectin in European and North American countries.[3–6] However, we are aware of only two patients with Ancylostoma spp. infection treated with ivermectin in Japan.[6,7] Herein, we present a case of creeping disease, probably caused by animal hookworms, successfully treated with ivermectin. We also report the results of microplate enzyme-linked immunosorbent assay (ELISA).

CASE REPORT

A 46-year-old-male Japanese office worker consulted our clinic, complaining of an itchy rash elongating by 1 cm per day on his right posterior thigh. He noticed the eruption after travelling to Indonesia. He denied eating any raw fish or meat, but admitted to walking along a river and in the jungle without shoes, and he had a history of leech bite. Creeping disease was suspected because of the typical clinical manifestation.

Serpiginous linear erythema, 2–3 mm wide, was distributed on the back of his right thigh (Fig. 1a). Pinhead-sized papules and vesicles were found at the edge of the erythema. The patient complained of pruritus. Laboratory examination did not reveal eosinophilia or elevation of immunoglobulin (Ig)E levels.

Three days after his first visit, the fresh linear erythema had elongated by approximately 3 cm (Fig. 1b). Ultrasonography did not show presence of the parasite. Histology showed moderate eosinophilic

Correspondence: Yuko Senba, M.D., Department of Dermatology, Mie University Graduate School of Medicine, 2-174, Edobashi, Tsu, Mie 514-8507 Japan. Email: senba-y@clin.medic.mie-u.ac.jp

Received 17 June 2008; accepted 27 October 2008.

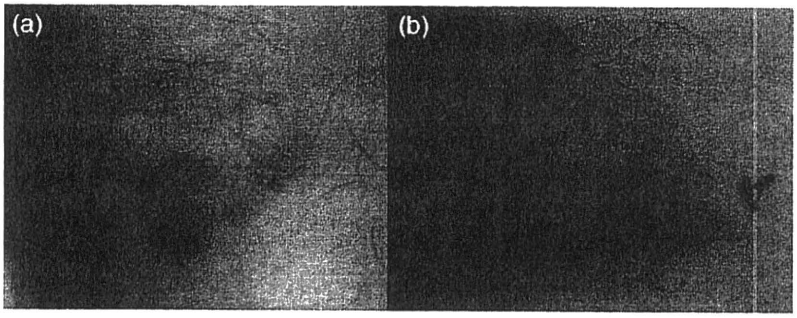

Figure 1. (a) A serpiginous linear erythema on the thigh. (b) A fresh erythema elongating approximately 3 cm long. A skin biopsy was taken from two different locations, indicated by the black arrows.

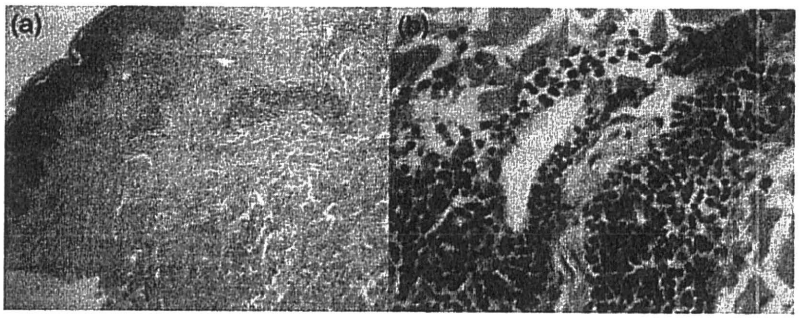

Figure 2. Perivascular eosinophilic infiltration in the dermis is noted. The parasite or the larva tract was not detected (original magnification: [a] ×40; [b] ×400).

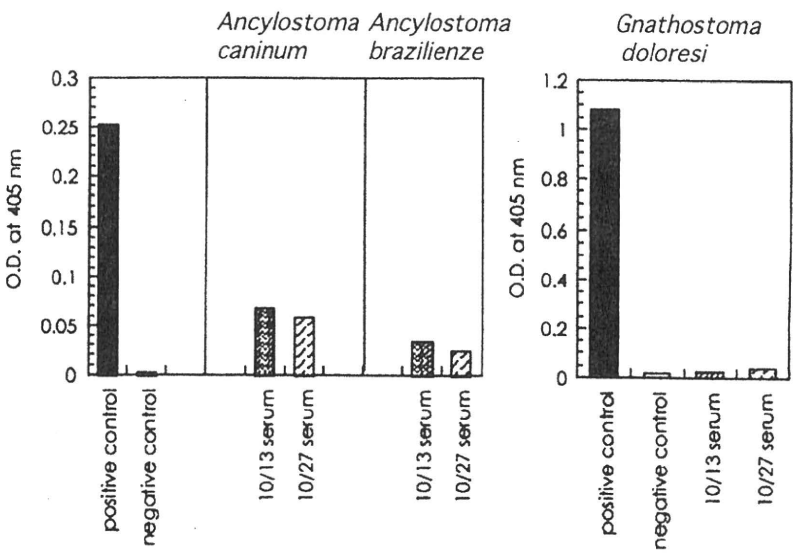

Figure 3. Specific immunoglobulin (Ig)G antibody titers in the sera were measured by microplate enzyme-linked immunosorbent assay using Necator americanus, Ancylostoma caninum and Gnathostoma doloresi. Significant elevation of the titers was not observed. (Positive control was serum from an ancylostomiasis patient in Papua New Guinea. Negative control was sera from healthy volunteers of Miyazaki University.)

infiltration around the small blood vessel. However, neither the body of the parasite nor a cleft indicating the larva tract were detectable (Fig. 2). We investigated the sera from the patient, sampled before and after the treatment. Specific IgG antibody titers in the sera were measured by microplate ELISA using human hookworm (Necator americanus), dog hookworm (Ancylostoma caninum) and Gnathostoma

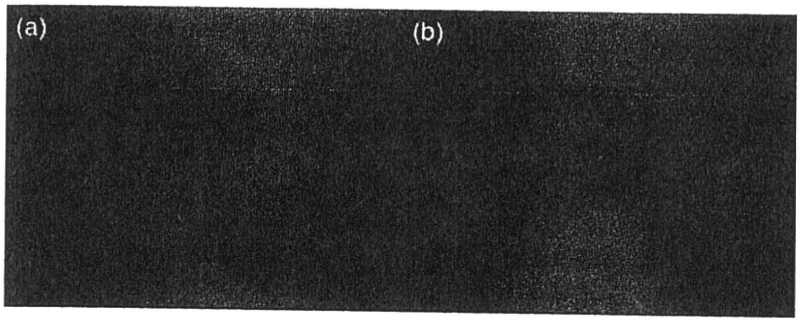

Figure 4. (a) Further elongation of fresh erythema. (b) A brown-colored pigmentation 4 days after taking ivermectin.

(Gnathostoma doloresi) (Fig. 3). Examination for Gnathostoma was negative. Antibody titers against N. americanus and A. caninum were above the negative control, although, compared with the positive control, immunoreactions of the patient's sera were weak. Because the titer was below 0.1 (optical density, 450 nm), we considered that elevation of the titer was not significant.

We diagnosed this case as creeping disease, because of the typical serpiginous erythema and a history of traveling in southeast Asia. Creeping disease caused by percutaneous infection such as A. canium and A. brasilliense was strongly suspected.

One week after the biopsy, further elongation of the worm tunnel was observed (Fig. 4a). A single oral dose of 200 μg/kg ivermectin between meals was then administered. Four days after taking ivermectin, the erythema faded (Fig. 4b). The pruritus resolved within 2 days of the administration. Neither adverse reaction nor recurrence was observed.

DISCUSSION

Creeping disease is an infectious skin disease caused by the larval form of nematodes. Our case was considered as a percutaneous larval hookworm infection. The patient had traveled to southeast Asia, where the main species is A. brasilliense, which is common in tropical areas, but A. canium and other canine species may also be the cause of the pathogen. According to Bouchaud et al.,[3] in cases of creeping disease with Ancylostoma spp., the incubation period is usually not more than 1 month, and pruritus was observed in all cases. The creeping eruption caused by A. brasilliense can resolve spontaneously in most cases, because the larvae are not able to complete their life cycle within humans and die after several months. However, our patient continued to suffer from severe pruritus, and was treated with a single oral dose of 200 μg/kg ivermectin. Previous reports state that the mean interval between ivermectin intake and the disappearance of pruritus is 3 days, and the mean interval between ivermectin therapy and the disappearance of lesions is 9 days.[3]

Ivermectin is a semisynthetic macrolide endectocide which has been often used against onchocerciasis and scabies.[2] Recently, several reports from Europe and North America have reported the efficacy of ivermectin against creeping disease. In a prospective study performed in France, 64 patients with creeping disease were enrolled and treated with a single 200 μg/kg dose of ivermectin taken between meals,[3] and 77% of them were cured. After one or two supplementary doses, the overall cure rate reached 97%. In a previous report by Caumes et al., a single 400 μg/kg dose of ivermectin was effective for all 10 patients.[4] Karavichian et al. reported that 17 patients were treated with a single 200 μg/kg dose of ivermectin, and 76% patients were cured.[5] However, we know of only two cases of creeping disease treated with ivermectin published in Japan.[6,7]

To confirm the diagnosis, it is necessary to detect the larvae in the biopsied specimen. But this is difficult because the parasite moves rapidly beyond the obvious lesion. Therefore, we measured the parasite-specific IgG antibody titers in the patient's sera by microplate ELISA. The elevation of the antibody titers, however, was not significant. Immunoserological examination is known to show negative

in most patients with A. brasilliense and A. canium infection, because hookworms are too small to cause sufficient immunoresponse and produce antibody.[8] According to Uchiyama et al., only three of seven suspected cases of Ancylostomas spp. infection showed seropositive against two hookworm antigens (N. americanus and A. caninum).[1] In contrast, in cases with Gnathostoma and Ascaris spp. infection, microplate ELISA is usually positive and has diagnostic significance.[9] Immunoserological examination may be of limited help in the diagnosis of creeping disease by Ancylostoma spp. and Ascaris spp. because it shows false-negative in many patients.

REFERENCES

1 Nakamura-Uchiyama F, Yamasaki E, Nawa Y. One confirmed and six suspected cases of cutaneous larva migrans caused by overseas infection with dog hookworm larvae. J Dermatol 2002; 29: 104–111.

2 Dourmishev AL, Dourmishev LA, Schwartz RA. Ivermectin: pharmacology and application in dermatology. Int J Dermatol 2005; 44: 981–988.

3 Bouchaud O, Houze S, Schiemann R et al. Cutaneous larva migrans in travelers: a prospective study, with assessment of therapy with ivermectin. Clin Infect Dis 2000; 31: 493–498.

4 Caumes E. Treatment of cutaneous larva migrans. Clin Infet Dis 2000; 30: 811–814.

5 Kravichian K, Nuchprayoon S, Sitichalernchai P, Chaicumpa W, Yentakam S. Treatment of cutaneous gnathostomiasis with ivermectin. Am J Trop Med Hyg 2004; 71(5): 623–628.

6 Kinoshita Y, Hara H, Ochiai T, Suzuki H, Morishima K, Nawa Y. [Creeping eruption caused by the larva of Ancylostoma brasilliense.] Hihukano-rinsyo 2003; 45(2): 125–127. (In Japanese.)

7 Murayama J, Ono H, Taniguchi H, Takino C, Ohtaki N, Akao N. Creeping eruption caused by the hookworm larva. Hihukano-rinsyo 2006; 48(5): 671–673 (in Japanese).

8 Nakamura-Uchiyama F. [Cutaneous larva migrans.] Hihukano-rinsyo 2004; 46(11): 1635–1645. (In Japanese.)

9 Maruyama H, Noda S, Choi WY, Ohta N, Nawa Y. Fine binding specificities to Ascaris suum and Ascaris lumbricoides antigens of the sera from patients of probable visceral larva migrans due to Ascaris suum. Parasitology Int 1997; 46: 181–188.

CASE REPORT

Circ J 2009; 73: 1344–1348

Fulminant Eosinophilic Myocarditis Associated With Visceral Larva Migrans Caused by Toxocara Canis Infection

Kenki Enko, MD; Takeshi Tada, MD; Keiko O. Ohgo, MD; Satoshi Nagase, MD; Kazufumi Nakamura, MD; Kei Ohta, MD*; Shingo Ichiba, MD*; Yoshihito Ujike, MD*; Yukifumi Nawa, MD**; Haruhiko Maruyama, MD**; Tohru Ohe, MD; Kengo F. Kusano, MD

A 19-year-old man was transferred to hospital because of myocarditis with cardiogenic shock. Echocardiography showed a left ventricular ejection fraction of 23.8% and an intermediate amount of pericardial effusion. The patient immediately received an intra-aortic balloon pump and percutaneous cardiopulmonary support. Right ventricular endomyocardial biopsy was performed in the acute phase and showed extensive eosinophilic inflammatory cell infiltration, severe interstitial edema and moderate myocardial necrosis. High-dose corticosteroids were administered. Because the patient's antibody titer against Toxocara canis was high and his symptoms had appeared after eating raw deer meat, the diagnosis was fulminant eosinophilic myocarditis caused by a hypersensitivity reaction to visceral larval migrans. After starting high-dose corticosteroids, the ejectionfraction dramatically improved, the eosinophilia decreased and the patient made a full recovery. (Circ J 2009; 73: 1344–1348)

Key Words: Corticosteroids; Eosinophilia; Myocarditis; Toxocara canis; Visceral larva migrans

Acute myocarditis occasionally progress to a fulminant course, which can be fatal without mechanical support. Most of these fulminant cases are caused by viral infection for which corticosteroids are not effective[1,2] Visceral larva migrans (VLM), described by Beaver et al in 1952[3] results mainly from infection by the common roundworms of dogs and cats, Toxocara (T.) canis and T. cati, respectively. Infection with the parasite usually causes marked eosinophilia and the development of eosinophilic-rich granulomatous lesions in the soft tissues of the body, including the myocardium[4,5] It has been reported that administration of high-dose corticosteroids in the early stage can dramatically improve eosinophilic myocarditis, but fulminant cases are usually diagnosed at autopsy. We report a rare case of fulminant eosinophilic myocarditis caused by a hypersensitivity reaction to VLM.

Case Report

A 19-year-old man presented at a local hospital complaining of chest discomfort and pain. He had been healthy with no significant preceding symptoms, allergic history or past medical history. ECG showed a slight ST elevation in all limb and precordial leads, except for aVR (Figure 1A). Chest X-ray showed cardiomegaly, pulmonary congestion

Table 1. Results of Blood Examination on Admission

Complete blood count	
WBC	22,900/μl
Neutrophils	72.2%
Lymphocytes	16.6%
Monocytes	6.6%
Eosinophils	4.6% (1,053/μl)
Basophils	0%
RBC	560×10⁴/μl
Hemoglobin	17.9 g/dl
Hematocrit	54.3%
Platelets	25.8×10⁴/μl
Blood chemistry	
Total bilirubin	3.09 mg/dl
Total protein	5.8 g/dl
Albumin	3.6 g/dl
AST	2,462 IU/L
ALT	2,967 IU/L
LDH	2,126 IU/L
CK	144 IU/L
Troponin T (+)	
BUN	24.7 mg/dl
Cr	1.21 mg/dl
UA	10.2 mg/dl
Na	130 mmol/L
K	4.9 mmol/L
Cl	100 mmol/L
CRP	4.0 mg/dl
ECP	54.9 ng/ml
Infection markers	
HBs-Ag	(–)
HCV-AB	(–)
STS	(–)
TPHA	(–)

WBC, white blood cells; RBC, red blood cells; AST, aspartate aminotransferase; ALT, alanine aminotransferase; LDH, lactate dehydrogenase; CK, creatine kinase; BUN, blood urea nitrogen; Cr, creatinine; UA, uric acid; CRP, C-reactive protein; ECP, eosinophil cationic protein; HBs-Ag, hepatitis B surface antigen; HCV, hepatitis C virus; TPHA, Treponema pallidum hemagglutination.

(Received April 4, 2008; revised manuscript received July 17, 2008; accepted July 23, 2008; released online December 27, 2008)
Departments of Cardiovascular Medicine, *Emergency and Critical Care Medicine, Okayama University Graduate School of Medicine, Dentistry, and Pharmaceutical Science, Okayama and **Department of Parasitology, Faculty of Medicine, University of Miyazaki, Miyazaki, Japan
Mailing address: Kengo F. Kusano, MD, Department of Cardiovascular Medicine, Okayama University Graduate School of Medicine, Dentistry, and Pharmaceutical Sciences, 2-5-1 Shikata-cho, Okayama 700-8558, Japan. E-mail: Kfuku0218@aol.com

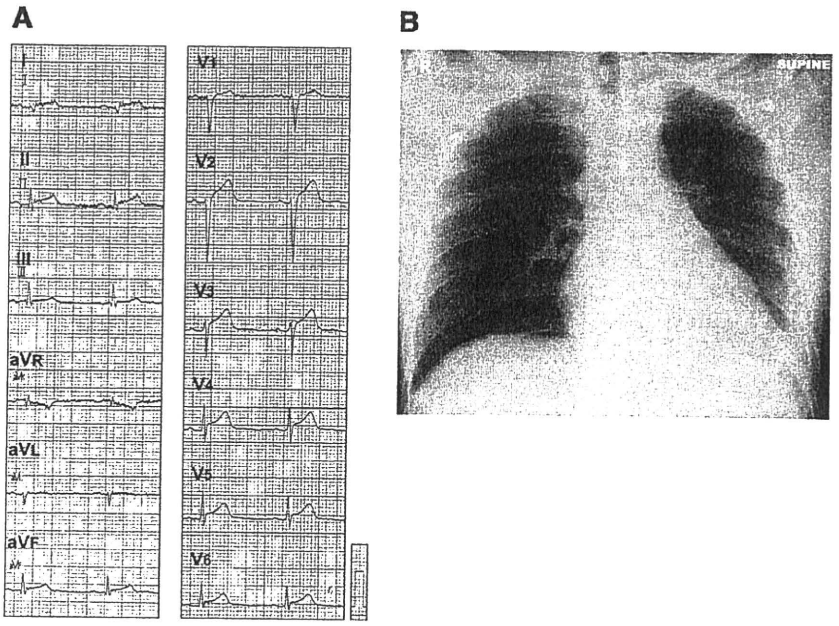

Figure 1. (A) Twelve-lead ECG on admission shows ST elevation. (B) Chest X-ray on admission shows the enlarged cardiac silhouette with pleural effusion.

Table 2. Viral Antibody Tests

Acute phase (admission)	Chronic phase (day 18)
Positive	Positive
Coxsackie virus A16 (×64)	Coxsackie virus A16 (×64)
Coxsackie virus B4 (×32)	Coxsackie virus B4 (×16)
Parainfluenza 3 (×40)	Parainfluenza 3 (×40)
Herpes simplex (×16)	Herpes simplex (×16)
Echo 12 (×32)	Echo 12 (×16)
Negative	Negative
Echo 3, 6, 7, 11	Echo 3, 6, 7, 11
Coxsakie virus A7	Coxsakie virus A7
Coxsakie virus B1, B2, B3, B5, B6	Coxsakie virus B1, B2, B3, B5, B6
Adenovirus, mumps virus, RS virus	Adenovirus, mumps virus, RS virus

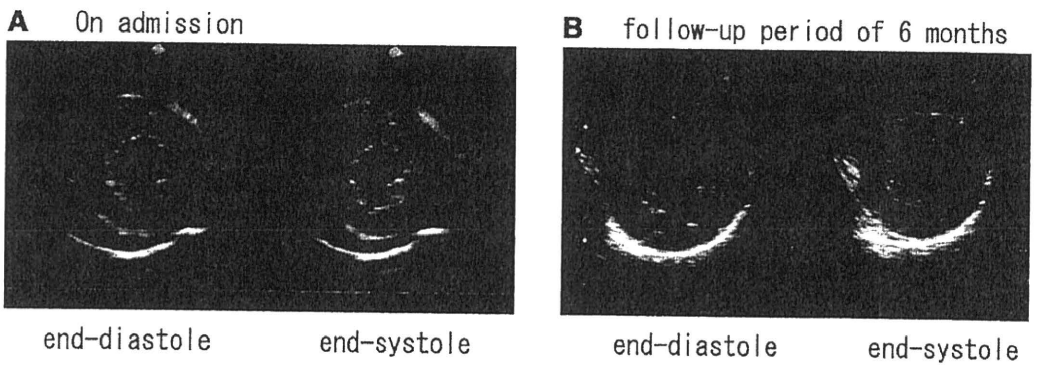

Figure 2. Echocardiography. (A) Large amount of pericardial effusion, wall thickening and severely decreased wall motion. (B) Six months after discharge, all abnormalities have improved dramatically.

and left pleural effusion (Figure 1B). He was admitted as an emergency with the suspicion of acute pericarditis. After admission, his general condition and left ventricular ejection fraction (LVEF) rapidly deteriorated and administration of dopamine was started because of cardiogenic shock. The next day he was transferred to our hospital for treatment of fulminant myo/pericarditis of unknown etiology.

On admission, his systolic blood pressure was 80 mmHg and heart rate was 130 beats/min with paradoxical pulse. A third heart sound was audible and his jugular vein was distended. Hematological and serological examinations (Table 1) showed marked increases in the total white blood cell count (22,900/μl) and eosinophil count (1,053/μl). C-reactive protein was also elevated (4.0 mg/dl), as was eosin-

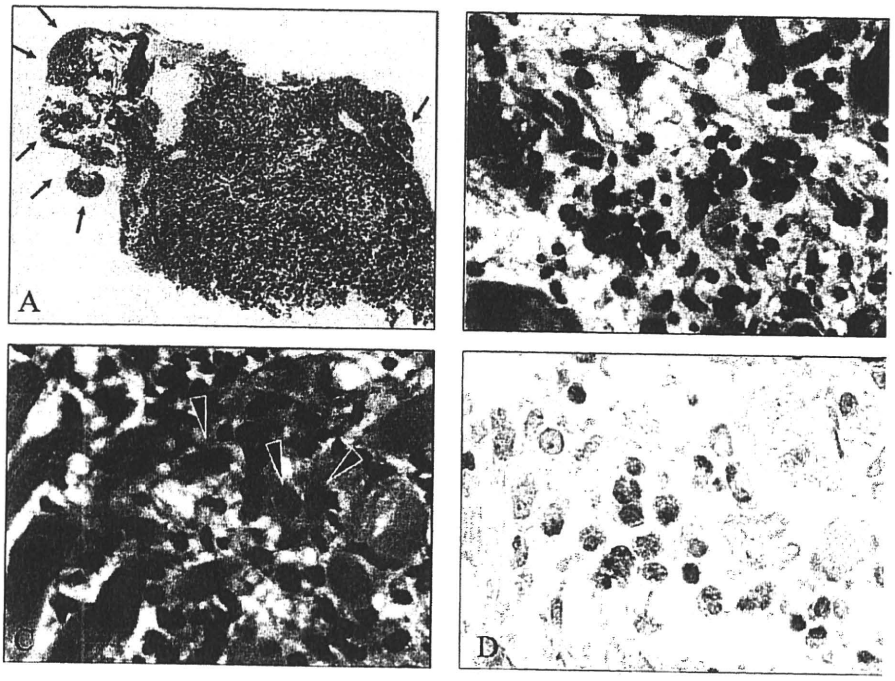

Figure 3. (A) Diffuse inflammatory infiltrate of the myocardium and endocardial involvement by mural thrombi containing eosinophils (arrows; H&E, ×25). (B) Eosinophil-rich inflammatory infiltrate with associated interstitial edema (H&E, ×200). (C) Interstitial Inflammatory infiltrated with associated myocyte necrosis (arrowheads; H&E, ×400). (D) Infiltrating eosinophils revealed by immunostaining with major basic protein (×400).

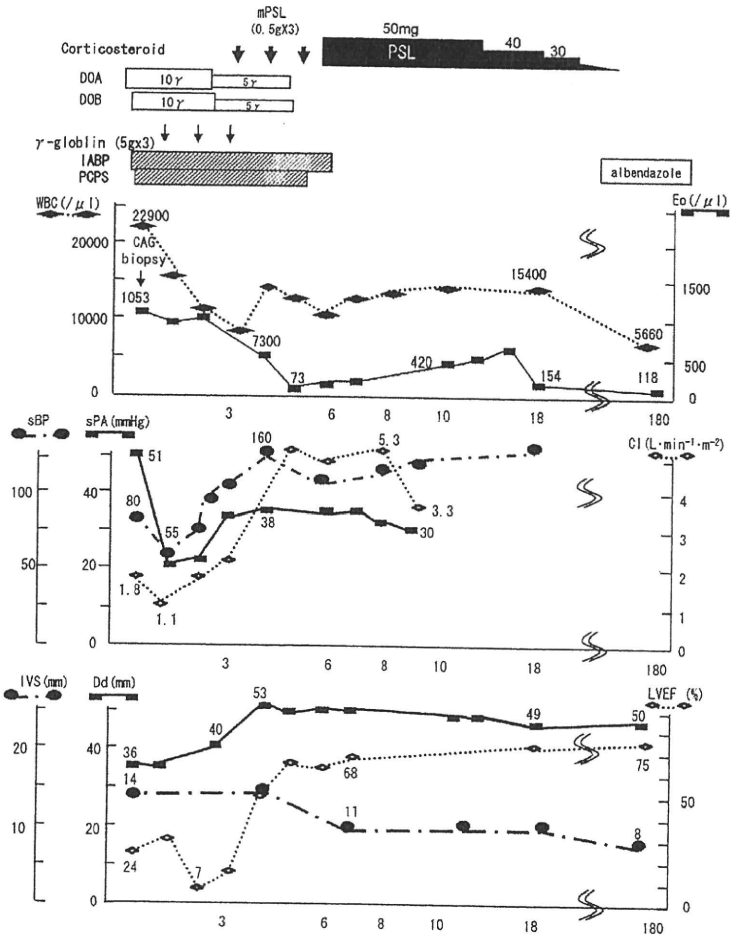

Figure 4. Clinical course. After starting corticosteroid treatment, LVEF and CI dramatically improved, with a decrease in the number of eosinophils. mPSL, methylprednisolone; PSL, prednisolone; DOA, dopamine; DOB, dobutamine; IABP, intra-aortic balloon pump; PCPS, percutaneous cardiopulmonary support; WBC, white blood cell count; Eo, eosinophil; sBP, systolic blood pressure; sPA, systolic pulmonary artery pressure; CI, cardiac index; IVS, interventricular septum; Dd, left ventricular end-diastolic dimension; LVEF, left ventricular ejection fraction.

ophilic cationic protein (ECP: 54.9 ng/ml; normal range: <14.7 ng/ml). Immunological examination on the first day of admission revealed positive antibody titers for Coxsackie virus A16, Coxsackie virus B4, parainfluenza 3, herpes simplex and echo 12 were positive, and negative titers for adenovirus, mumps, Coxsackie virus, echovirus (except for type 12), herpes simplex, parainfluenza, and RS virus. However, there was no significant change in the antibody titers in the tests performed in the chronic phase, which ruled out the active phase of viral infection (Table 2).

Echocardiography showed severe hypokinesis of the left ventricular wall motion (LVEF: 23.8%), with thickening of the left ventricle and a large amount of pericardial effusion (Figure 2A). A diagnosis of fulminant myocarditis with cardiogenic shock was made. An intra-aortic balloon pump (IABP) and percutaneous cardiopulmonary support (PCPS) were immediately inserted and cardiac catheterization was then performed to decide the course of treatment.

Coronary angiography revealed no stenotic lesions. Right heart catheterization showed a pulmonary artery systolic pressure of 51 mmHg, pulmonary artery wedge pressure of 20 mmHg, and right atrial pressure 18 mmHg. Right ventricular endomyocardial biopsy was performed and histopathology revealed extensive interstitial edema with diffuse inflammatory interstitial infiltrate and myocardial necrosis. The infiltrating cells were eosinophils that had partially degranulated. These findings were compatible with acute eosinophilic myocarditis (Figure 3).

We started intravenous methylprednisolone at 500 mg/day for 3 days, followed by oral administration of prednisolone at 50 mg/day. After starting corticosteroid therapy, his ventricular function dramatically improved and the eosinophil count decreased promptly and normalized. On day 6 (day 1 is date of admission), the IABP and PCPS were removed (Figure 4) and prednisolone was tapered over a period of 8 weeks.

The patient has been doing well without any cardiac events since discharge and echocardiographic findings have remained normal during follow-up of 6 months (Figure 2B).

Anti-IgG to T. canis was detected in his serum by a commercial multiple-dot ELISA kit (SRL, Tokyo, Japan), although we could not find evidence of the parasites in the myocardial biopsy. Therefore, we performed further examination at the Department of Parasitology, Miyazaki Medical University, Miyazaki, Japan. Binding of patient serum to parasite antigens was tested using ELISA. Briefly, wells of microtiter plates were coated with 10 μg/ml of T. canis larval excretory–secretory antigen, and incubated with diluted samples (1:900–1:2,700). Binding of antibodies to T. canis antigen was detected with horse-radish peroxidase-conjugated anti human IgG and optical densities were read with a microplate reader (BioRAD). The patient had eaten raw deer meat 1 week before admission, so the final diagnosis was fulminant eosinophilic myocarditis caused by a hypersensitivity reaction to VLM after T. canis infection. We got the result 4 months after he had been discharged and prescribed albendazole (600 mg/day), which was continued for 4 weeks without any adverse effect.

Discussion

Acute fulminant eosinophilic myocarditis is a rare disorder of unknown etiology, frequently resulting in cardiogenic shock and a fatal clinical course. Predisposing factors include viral infection, history of allergic diathesis, and initiation of new medications[6] It has been suggested[7] that there are 3 clinical stages of eosinophilic myocarditis: acute necrotizing phase, thrombotic phase and endomyocardial fibrosis phase. Loffler's endomyocarditis is considered to correspond to the second stage of eosinophilic endomyocardial disease. The third stage probably corresponds to restrictive myocarditis. Differential diagnoses include other types of myocarditis, Churg-Strauss syndrome, hypersensitivity reaction, malignant diseases, parasitic infection or hypereosinophilic syndrome. Eosinophilic myocarditis associated with hypereosinophilic syndrome is usually less acute and less severe than acute fulminant necrotizing eosinophilic myocarditis[8] In the present case, the pathological findings were compatible with fulminant necrotizing eosinophilic myocarditis.

Because the symptoms of the patient appeared after eating raw deer meat and because the antibody titer against T. canis was high, we made a final diagnosis of eosinophilic myocarditis associated with VLM because of T. canis infection. T. canis, the common dog roundworm, is 1 of the causative agents of VLM. When embryonated eggs of T. canis from contaminated meat reach the human gastrointestinal tract, they hatch and enter the portal system, reaching the liver. Some larvae then migrate to the lungs and heart through the systemic circulation[9,10] A previous case of myocarditis associated with VLM has been reported[11] and another in Japan[12] so the present case is a very rare occurrence. Although the Myocarditis Treatment Trial found no statistical advantage of corticosteroid treatment in biopsy-proven myocarditis (Dallas Criteria)[2] it has been suggested that eosinophilic heart disease may be a subset with greater responsiveness[1] to corticosteroids. However, acute fulminant eosinophilic myocarditis is usually fatal and antemortem diagnosis is difficult. Corticosteroid therapy in the early stage can have favorable effect if early diagnosis by endomyocardial biopsy is made. In the present case, endomyocardial biopsy in the acute phase was helpful for diagnosis and therapeutic decision-making. Necrotizing eosinophilic myocarditis associated with VLM is very rare, but it should be taken into consideration.

Albendazole is a benzimidazole anthelmintic and is used as treatment for various parasitic infections. The mechanism of its anthelmintic action is inhibition of tubulin polymerization and microtubule-dependent glucose uptake inhibition. It has been reported that the incidence of adverse effects of albendazole is 23% and that the main adverse effect is liver injury (16%)[13] We were able to continue albendazole treatment of the present patient for 4 weeks without any adverse effects. Prompt anthelmintic treatment for parasite infection is recommended in eosinophilic myocarditis associated with VLM, so we should have administered albendazole earlier in the clinical course.

The patient was thought to be complicated by cardiac tamponade on admission, so PCPS was immediately inserted because of rapid worsening of left ventricular contraction and cardiogenic shock. The patient became hemodynamically stable with the PCPS and pericardial effusion decreased dramatically after starting corticosteroid therapy, so we did not perform pericardiocentesis on admission, which we probably should have done.

References

1. Jones SR, Herskowitz A, Hutchins GM, Bauqhman KL. Effects of immunosuppressive therapy in biopsy-proved myocarditis and borderline myocarditis on left ventricular function. Am J Cardiol 1991;

68: 370–376.
2. Mason JW, O'Connell JB, Herskowitz A, Rose NR, McManus BM, Billinqham ME, et al. A clinical trial of immunosuppressive therapy for myocarditis: The Myocarditis Treatment Trial Investigators. N Engl J Med 1995; 333: 269–275.
3. Beaver PC, Snyder CH, Carrera GM, Dent JH, Lafferty JW. Chronic eosinophilia due to visceral larva migrans: Report of three cases. Pediatrics 1952; 9: 7–19.
4. Dent JH, Nichols RL, Beaver PC, Carrera GM, Staggers RJ. Visceral larva migrans with a case report. Am J Pathol 1956; 32: 777–803.
5. Cookston M, Stober M, Kayes SG. Eosinophilic myocarditis in CBA/J mice infected with Toxocara canis. Am J Pathol 1990; 136: 1137–1145.
6. Watanabe N, Nakagawa S, Fukunaga T, Fukuoka S, Hatakeyama K, Hayashi T. Acute necrotizing eosinophilic myocarditis successfully treated by high dose methylprednisolone. Jpn Circ J 2001; 65: 923–926.
7. Brockington IF, Olsen EG. Eosinophilia and endomyocardial fibrosis. Postgrad Med J 1972; 48: 740–741.
8. Cooper LT, Zehr KJ. Biventricular assist device placement and immunosuppression as therapy for necrotizing eosinophilic myocarditis. Nat Clin Pract Cardiovasc Med 2005; 2: 544–548.
9. Mok CH. Visceral larva migrans: A discussion based on review of the literature. Clin Pediatr (Phil) 1968; 7: 565–573.
10. Woodruff AW. Toxocariasis. BMJ 1970; 3: 663–669.
11. Vargo TA, Singer DB, Gillatte PC, Fernbach DJ. Myocarditis due to visceral larva migrans. J Pediatr 1977; 90: 322–323.
12. Abe K, Shimokawa H, Kubota T, Nawa Y, Takeshita A. Myocarditis associated with visceral larva migrans due to Toxocara canis. Intern Med 2002; 41: 706–708.
13. Drugs in Japan Forum. Drugs in Japan 2007; 209–210.

THE JOURNAL OF BIOLOGICAL CHEMISTRY VOL. 284, NO. 11, pp. 7255–7263, March 13, 2009

Novel Mitochondrial Complex II Isolated from *Trypanosoma cruzi* Is Composed of 12 Peptides Including a Heterodimeric Ip Subunit*[S]

Received for publication, August 26, 2008, and in revised form, January 2, 2009 Published, JBC Papers in Press, January 2, 2009, DOI 10.1074/jbc.M806623200

Jorge Morales[‡1], Tatsushi Mogi[‡2], Shigeru Mineki[§], Eizo Takashima[‡3], Reiko Mineki[¶], Hiroko Hirawake[‡], Kimitoshi Sakamoto[‡], Satoshi Ōmura[‖], and Kiyoshi Kita[‡4]

From the [‡]Department of Biomedical Chemistry, Graduate School of Medicine, the University of Tokyo, Hongo, Bunkyo-ku, Tokyo 113-0033, the [§]Department of Applied Biological Science, Faculty of Science and Technology, Tokyo University of Science, Noda, Chiba 278-8510, the [¶]Division of Proteomics and BioMolecular Science, Juntendo University Graduate School of Medicine, Hongo, Bunkyo-ku, Tokyo 113-8421, and the [‖]Kitasato Institute for Life Sciences and Graduate School of Infection Control Sciences, Kitasato University, Minato-ku, Tokyo 108-8641, Japan

Mitochondrial respiratory enzymes play a central role in energy production in aerobic organisms. They differentiated from the α-proteobacteria-derived ancestors by adding non-catalytic subunits. An exception is Complex II (succinate: ubiquinone reductase), which is composed of four α-proteobacteria-derived catalytic subunits (SDH1–SDH4). Complex II often plays a pivotal role in adaptation of parasites in host organisms and would be a potential target for new drugs. We purified Complex II from the parasitic protist *Trypanosoma cruzi* and obtained the unexpected result that it consists of six hydrophilic (SDH1, $SDH2_N$, $SDH2_C$, and SDH5–SDH7) and six hydrophobic (SDH3, SDH4, and SDH8–SDH11) nucleus-encoded subunits. Orthologous genes for each subunit were identified in *Trypanosoma brucei* and *Leishmania major*. Notably, the iron-sulfur subunit was heterodimeric; $SDH2_N$ and $SDH2_C$ contain the plant-type ferredoxin domain in the N-terminal half and the bacterial ferredoxin domain in the C-terminal half, respectively. Catalytic subunits (SDH1, $SDH2_N$ plus $SDH2_C$, SDH3, and SDH4) contain all key residues for binding of dicarboxylates and quinones, but the enzyme showed the lower affinity for both substrates and inhibitors than mammalian enzymes. In addition, the enzyme binds protoheme IX, but SDH3 lacks a ligand histidine. These unusual features are unique in the Trypanosomatida and make their Complex II a target for new chemotherapeutic agents.

The parasitic protist *Trypanosoma cruzi* is the etiological agent of Chagas disease, a public health threat in Central and South America. These parasites are normally transmitted by reduviid bugs via the vector feces after a bug bite and also via transfusion of infected blood. About 16–18 million people are infected, and 100 million are at risk, but there are no definitive chemotherapeutic treatments available (1). Despite having potential pathways for oxidative phosphorylation (2), all trypanosomatids (*Trypanosoma* and *Leishmania* species) analyzed so far are characterized by incomplete oxidation of glucose with secretion of end products, such as succinate, alanine, ethanol, acetate, pyruvate, and glycerol (3, 4) (Fig. 1). Major routes for formation of succinate in *Trypanosoma brucei* are via NADH-dependent fumarate reductase in glycosomes and mitochondria (5, 6). In trypanosomatid mitochondria, the Krebs cycle is inefficient, and pyruvate is principally converted to acetate via acetate:succinate CoA transferase (7). A part of the Krebs cycle operates the utilization of histidine in the insect stage of *T. cruzi* (8).

Mitochondrial Complex II (succinate:quinone reductase (SQR)[5] and succinate dehydrogenase (SDH)) serves as a membrane-bound Krebs cycle enzyme and often plays a pivotal role in adaptation of parasites to environments in their host (9, 10). In general, Complex II consists of four subunits (11). A flavoprotein subunit (SDH1, Fp) and an iron-sulfur subunit (SDH2, Ip) form a soluble heterodimer, which then binds to a membrane anchor heterodimer, SDH3 (CybL) and SDH4 (CybS). SDH1 contains a covalently bound FAD and catalyzes the oxidation of succinate to fumarate. SDH2 transfers electrons to ubiquinone via the [2Fe-2S] cluster in the N-terminal plant-type ferredoxin domain (Ip_N) and the [4Fe-4S] and [3Fe-4S] clusters in the C-terminal bacterial ferredoxin domain (Ip_C). Ubiquinone is bound and reduced in a pocket provided by SDH2, SDH3, and SDH4 (12–14). SDH3 and SDH4 contain three transmembrane helices and coordinate protoheme IX via histidine in the second helices of each subunit (11–14).

* This work was supported in part by Grant-in-aid for Scientific Research 20570124 (to T. M.), Creative Scientific Research Grant 18GS0314 (to K. K.), Grant-in-aid for Scientific Research on Priority Areas 18073004 (to K. K.) from the Japanese Society for the Promotion of Science, and Targeted Proteins Research Program (to K. K.) from the Japanese Ministry of Education, Science, Culture, Sports and Technology (MEXT). The costs of publication of this article were defrayed in part by the payment of page charges. This article must therefore be hereby marked "*advertisement*" in accordance with 18 U.S.C. Section 1734 solely to indicate this fact.

[S] The on-line version of this article (available at http://www.jbc.org) contains supplemental Table S1.

[1] Supported by a Japanese Government scholarship from Ministry of Education, Science, Culture, Sports and Technology.

[2] To whom correspondence may be addressed. Tel.: 81-3-5841-3526; Fax: 81-3-5841-3444; E-mail: tmogi@m.u-tokyo.ac.jp.

[3] Present address: Dept. of Microbiology, School of Life Dentistry at Tokyo, Nippon Dental University, Tokyo 102-8159, Japan.

[4] To whom correspondence may be addressed. Tel.: 81-3-5841-3526; Fax: 81-3-5841-3444; E-mail: kitak@m.u-tokyo.ac.jp.

[5] The abbreviations used are: SQR, succinate:quinone reductase; hrCNE, high resolution clear native electrophoresis; IC_{50}, the 50% inhibitory concentration; Ip_N, the N-terminal plant-type ferredoxin domain; Ip_C, the C-terminal bacterial ferredoxin domain; DCIP, 2,4-dichlorophenolindophenol; SML, sucrose monolaurate; Tricine, *N*-[2-hydroxy-1,1-bis(hydroxymethyl)ethyl]-glycine; MOPS, 3-(*N*-morpholino)propanesulfonic acid; Q_n, ubiquinone-*n*.

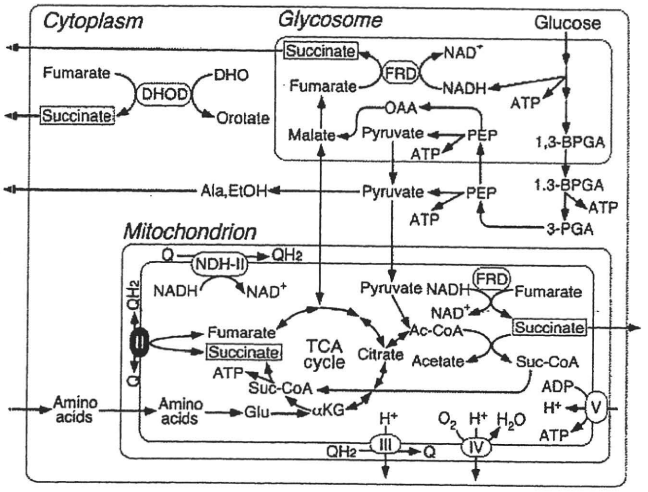

FIGURE 1. **Metabolic pathways in *T. cruzi*.** Incomplete oxidation of glucose takes place in glycosomes and mitochondria, and end products such as succinate, L-alanine, ethanol, and acetate are excreted from parasites (3, 4). Cytoplasmic dihydroorotate (*DHO*):fumarate reductase (*DHOD*) contributes succinate production (6).

Parasitic nematodes adapted to hypoxic host environments often have modified respiratory chains. Many adult parasites perform fumarate respiration by expressing a stage-specific isoform of Complex II (9, 10). *Hemonchus contortus* uses an isoform for SDH2 (9), whereas *Ascaris suum* uses isoforms for SDH1 and SDH4 (10). To explore the adaptive strategy in a parasitic protist, we isolated mitochondria from axenic culture of *T. cruzi* epimastigotes and characterized the purified Complex II. Our results demonstrated for the first time that *T. cruzi* Complex II is an unusual supramolecular complex with a heterodimeric iron-sulfur subunit and seven novel noncatalytic subunits. Purified enzyme showed reduced binding affinities for both substrates and inhibitors. Because this novel structural organization is conserved in all trypanosomatids (2, 15, 16), parasite Complex II would be a potential target for the development of new chemotherapeutic agents for trypanosomiasis and leishmaniasis.

EXPERIMENTAL PROCEDURES

Preparation of Mitochondria—T. cruzi strain Tulahuhen was grown statically for 6–7 days at 26 °C in 300-cm^2 cell culture flasks (Falcon, BD Biosciences) containing 250 ml of the modified LIT medium (17), supplemented with 0.1% (w/v) glucose, 0.001% (w/v) hemin (Sigma), and 5% (v/v) fetal bovine serum (MP Biochemicals). Mitochondria were isolated from epimastigotes by the differential centrifugation method (18) with slight modifications. Parasites grown to $6-8 \times 10^7$ cells/ml were washed with buffer A (20 mM Tris-HCl, pH 7.2, 10 mM NaH_2PO_4, 1 mM sodium EDTA, 1 mM dithiothreitol, 0.225 M sucrose, 20 mM KCl, and 5 mM $MgCl_2$). Cells were disrupted by grinding with silicon carbide (Carborundum 440 mesh; Nacalai Tesque, Kyoto, Japan) in the presence of a minimum volume of buffer B (25 mM Tris-HCl, pH 7.6, 1 mM dithiothreitol, 1 mM sodium EDTA, 0.25 M sucrose, and EDTA-free Complete protease inhibitor mixture (Roche Applied Science)). The resultant cell paste was resuspended in buffer B and centrifuged at 500 × *g* for 5 min and 1000 × *g* for 15 min to remove silicon carbide and nuclear fraction, respectively. The mitochondrial fraction was recovered upon centrifugation of the last supernatant at 10,000 × *g* for 15 min, washed three times in buffer B, and resuspended to a protein concentration of ~30 mg/ml and kept at −80 °C until use.

TABLE 1
Purification of complex II from *T. cruzi* mitochondria

Step	Protein	Succinate:DCIP reductase	Yield	Purification
	mg	*units*	*units/mg*	*%*	*-fold*
Mitochondria	314	27	0.085	100	1.0
SML extract	141	22	0.16	83	1.9
Source 15Q	7.8	7.6	0.97	28	12
Superdex 200 (1st)	1.3	1.4	1.09	5.3	13
Superdex 200 (2nd)	0.15	0.43	2.87	1.6	34

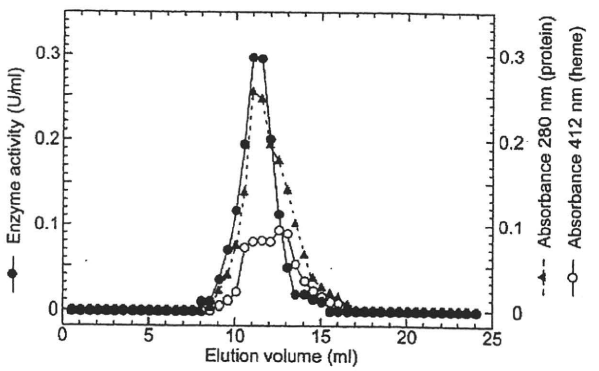

FIGURE 2. **Elution profile of *T. cruzi* Complex II on Superdex 200 chromatography.** Complex II fractions from the first gel filtration chromatography with a Superdex 200-pg column were concentrated and rechromatographed at the flow rate of 0.25 ml/min. Aliquots were collected every 0.5 ml. Elution profiles for proteins and cytochromes were monitored at 280 (▲) and 412 nm (○), respectively, and the enzyme activity (●) was measured as decylquinone-mediated succinate:DCIP reductase.

Isolation of Complex II—All steps were carried out at 4 °C. Mitochondrial fraction (~300 mg of protein from 10 liters culture) was brought to 70 ml with buffer C (10 mM KP_i, pH 7.5), 1 mM sodium EDTA, 1 mM sodium malonate, EDTA-free Complete protease inhibitor mixture (Roche Applied Science) (2 tablets/50 ml), 1% (w/v) sucrose monolaurate SM-1200 (SML) (Mitsubishi-Kagaku Foods Co., Tokyo, Japan)). The mixture was stirred for 30 min and centrifuged at 200,000 × *g* for 1 h. The supernatant was loaded at 1 ml/min onto a Source 15 Q column (1.6 inner diameter × 10 cm; GE Healthcare), equilibrated with buffer C containing 0.1% SML. After washing with 5 volumes of the same buffer, proteins were eluted with a 200-ml linear gradient of NaCl from 0 to 150 mM at 2 ml/min. Active fractions were concentrated to ~250 μl by ultrafiltration with Amicon Ultra-4 (molecular weight cutoff 100,000, Millipore) and subjected to gel filtration FPLC with a Superdex 200-pg 10/300 GL column (1 cm inner diameter × 30 cm; GE Healthcare) at 0.25 ml/min in 20 mM MOPS-NaOH, pH 7.2, containing 1 mM sodium EDTA, 1 mM sodium malonate, 150 mM NaCl, and 0.1% SML. Peak fractions were rechromatographed as above, and purified enzyme was concentrated and stored at −80 °C until use.

Identification of Complex II Subunits—The purified enzyme was subjected to 12.5% SDS-PAGE, and subunits were transferred to an Immobilon-P membrane (Millipore), followed by

staining with Coomassie Brilliant Blue R-250 (19, 20). Five or ten N-terminal amino acid residues were determined with a Procise 494 HT (Applied Biosystems) or an Hp G1005A (Hewlett-Packard Co.) Protein Sequencing System at the Bio-Medical Research Center of Juntendo University or APRO Life Science Institute, Inc. (Tokushima, Japan). When the N terminus was blocked, protein bands were digested with trypsin, and internal peptide sequences were determined (20). Genes coded for Complex II subunits were identified with BLASTP in the *T. cruzi* genome data base (15).

Phase Partitioning of Mitochondrial Fraction with Triton X-114—Phase partitioning by Triton X-114 was performed as described previously (21) with a slight modification. A total of 2–3 mg of mitochondrial fraction was resuspended in 1 ml of Tris-HCl, pH 7.5, 150 mM NaCl, 1 mM EDTA, 2 mM sodium malonate, Complete protease inhibitors mixture (Roche Applied Science) (2 tablets/50 ml), protease inhibitors mixture for mammalian cell and tissue extracts (Sigma) (10 μl/ml), and 2% (v/v) Triton X-114. The mixture was incubated for 30 min on ice and kept at −30 °C overnight. After thawing, the insoluble material was removed by centrifugation at 4 °C, and the supernatant was incubated for 10 min at 37 °C and centrifuged at 2000 × *g* for 10 min to separate the aqueous and detergent-rich phases. The aqueous phase was brought to 2% (v/v) Triton X-114, whereas the detergent-rich fraction was brought to 1 ml with the above buffer. After incubation on ice for 10 min, samples were incubated at 37 °C for 10 min and phases separated as before. This wash step was repeated three times. Finally, the samples were dialyzed and concentrated by Amicon Ultra-4 (Millipore) in the presence of 50 mM imidazole, 50 mM NaCl, 6 mM aminocaproic acid, 0.05% (w/v) deoxycholate, and 0.1% (w/v) SML, pH 7, and kept at −80 °C until use.

Enzyme Assay—Decylubiquinone-mediated succinate-2,4 dichlorophenolindophenol (DCIP) reductase activity was measured at 25 °C in 100 mM potassium phosphate, pH 7.4, containing 1 mM $MgCl_2$, 2 mM KCN, 0.1 mM antimycin A (Sigma), and 0.1% SML with 63 μM decylubiquinone (Sigma) *plus* 60 μM DCIP. After 2 min of incubation, reduction of DCIP (ϵ_{600} = 21 mM^{-1} cm^{-1}) was measured in the presence of 10 mM succinate. SQR activity was determined with 40 μM ubiquinone-2 (Q_2) (Sigma, ϵ_{278} = 12.3 mM^{-1} cm^{-1}). Kinetic analysis was done with KaleidaGraph version 4.0 (Synergy Software).

Miscellaneous—High resolution clear native electrophoresis (hrCNE) (22) was performed with 4–16% Novex gels (Invitrogen) using 0.02% dodecylmaltoside and 0.05% sodium deoxycholate for the cathode buffer additives, and the Complex II band was visualized by the activity staining (23) or Coomassie Brilliant Blue. Tricine-PAGE analysis was done with Novex 10–20% Tricine gels (Invitrogen), and proteins bands were sequentially stained by Sypro ruby (Invitrogen) and silver. During purification the succinate-decylubiquinone-DCIP reduc-

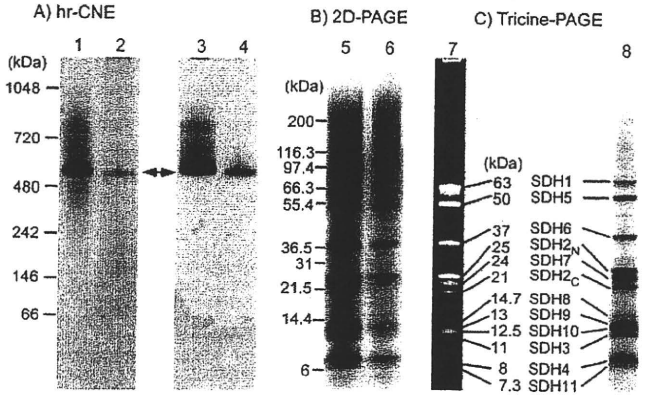

FIGURE 3. **Electrophoresis analysis of *T. cruzi* Complex II.** *A*, purified Complex II (2 μg; *lanes 1* and *3*) and the detergent-rich fraction from the phase partitioning by Triton X-114 of the mitochondrial fraction (60 μg; *lines 2* and *4*) were subjected to hrCNE. Proteins were stained by Coomassie Brilliant Blue (*left panel*), and Complex II was visualized by SDH activity staining (*right panel*). *B*, proteins of Complex II showing SDH activity in *A* were analyzed by 10–20% Tricine SDS-PAGE and visualized by silver stain (*lane 5*, pure complex; *lane 6*, detergent-rich fraction). *C* shows the subunit composition of the pure Complex II from *T. cruzi* stained by SYPRO ruby (*lane 7*) or silver stain (*lane 8*). Molecular weight standards used are NativeMark (Invitrogen, *lane 1*) and Mark 12 unstained standards (Invitrogen, *lanes 5* and *7*).

TABLE 2
Identification of genes encoding subunits for *T. cruzi* complex II

Subunit[a]	Sequence confirmed[b]	Accession number or RefSeq ID at NCBI (haplotype,[c] M_r)	Identity[d]	TM[e]
			%	
SDH1	Ser^{10}–Met^{19}	AB031741 (NE, 66,974), XP_809281 (E, 18,231)	59	0
SDH5	Ala^{10}–Leu^{19}	XP_818124 (NE, 53,831), XP_810172 (E, 20,788)	16	0
$SDH2_N$	Ser^{188}–Arg^{196}, Lys^{201}–Ile^{204}, Gly^{221}–Asn^{223}, Glu^{267}–Ile^{269}	XP_814994 (merged, 32,232)[f]	24 (37)	0
$SDH2_C$	Pro^{2}–Leu^{6}	XP_803796 (NE, 21,352), XP_806126 (E, 21,379)	25 (43)	0
SDH6a	Val^{19}–Val^{28}	XP_809065 (NA, 36,077), XP_812789 (NA, 36,035)	15	0
SDH6b	Val^{19}–Val^{28}	XP_813603 (NA, 36,133), XP_813645 (NA, 36,039)	14	0
SDH7	Ile^{26}–Leu^{35}	XP_813318 (NE, 28,218), XP_820239 (E, 28,202)	22	0
SDH3	Val^{2}–Phe^{11}	XP_809410 (NE, 12,176), XP_810064 (E, 12,204)	29	1
SDH4	Phe^{39}–Thr^{48}	XP_808211 (E, 13,957), XP_816430 (NE, 13,975)	27	2
SDH8	Gly^{5}–Met^{16}	XP_809192 (NE, 16,199), XP_817545 (E, 16,143)	ND[g]	2
SDH9	Ile^{10}–Pro^{19}	XP_807105 (merged, 15,736)	ND	1
SDH10	Pro^{25}–Val^{33}	XP_808894 (NE, 15,565), XP_808903 (E, 15,554)	ND	1
SDH11	Phe^{20}–Cys^{29}	XP_814088 (E, 10,346), XP_814509 (NE, 10,337)	ND	1

[a] Alleles were named as SDH3-1 (XP_809410) and SDH3-2 (XP_810064) in the order of the accession numbers, except for SDH5.
[b] These are N-terminal sequences except for $SDH2_N$ and SDH8, where the N-terminal residues were blocked.
[c] Homozygous alleles located in a merged assembly of Esmeraldo (E) and non-Esmeraldo (NE) homologous sequences whose different copies were merged genes during the genome assembly are indicated by "merged." Haplotypes for gene with more than two copies in the genome that does not belong to a merged region are not assigned (NA).
[d] Identity % to counterparts in human were as follows: SDH1 (D30648), SDH2 (P21912), SDH3 (Q99643), or SDH4 (O14521). In parentheses, the identity % of $SDH2_N$ and $SDH2_C$ that correspond to either Met^{1}–Pro^{155} (Ip_N domain) or Tyr^{156}–Val^{280} (Ip_C domain), respectively, of human SDH2 is shown. Identity % for truncated forms of SDH1 and SDH5 (SDH1-2 and SDH5-2) in the Esmeraldo haplotype was 66 and 20%, respectively.
[e] Transmembrane segments (TM) were estimated with TMHMM (52) and SOSUI (53).
[f] SDH2N from other trypanosomatids lack Met^{1} to Arg^{42} of $TcSDH2_N$.
[g] ND indicates not determined because these hydrophobic sequences are a highly divergent form of mammalian sequences.

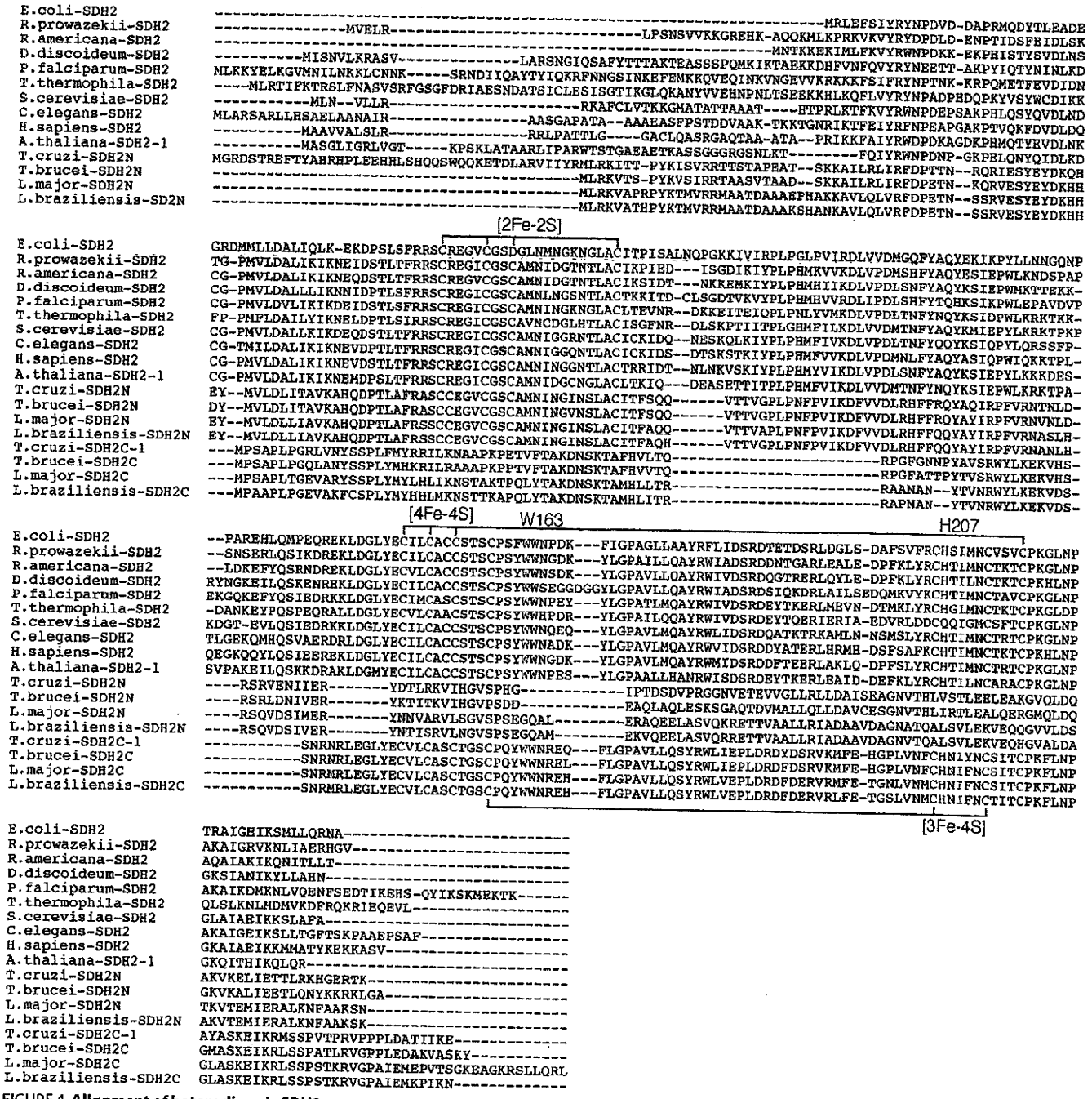

FIGURE 4. **Alignment of heterodimeric SDH2 sequences.** Amino acid residues proposed for binding of the iron-sulfur clusters are shown in *red* and those for the quinone binding in *blue*. Residue numbers refer to the *E. coli* SDH2 (SdhB) sequence. GenBank™ accession numbers for $SDH2_N$ and $SDH2_C$ sequences used are *T. cruzi* (XP_814994 and XP_803796), *T. brucei* (XP_847169 and XP_826981), and *L. major* (XP_001683488 and XP_001682013). Other SDH2 sequences used are *E. coli* (NP_415252), *Rickettsia prowazekii* (Q9ZEA1), *Reclinomonas americana* (NP_044798), *Dictyostelium discoideum* (XP_646559), *Plasmodium falciparum* (D86574), *Tetrahymena thermophila* (XP_001024894), *S. cerevisiae* (NP_012774), *Caenorhabditis elegans* (NP_495992), *H. sapiens* (NP_002991), and *A. thaliana* (NP_189374).

tase activity was monitored in a microplate spectrophotometer (Benchmark Plus, Bio-Rad). Kinetics and UV-visible absorption spectra were determined at room temperature with a V-660 UV-visible spectrophotometer (Jasco, Tokyo, Japan). Protoheme IX and protein concentrations were determined by pyridine hemochromogen method (24) and the micro BCA method (Pierce), respectively. Sequence alignment was done with ClustalX 2.0 (25).

RESULTS AND DISCUSSION

Isolation of T. cruzi Complex II—To determine the molecular organization of *T. cruzi* Complex II, we purified this enzyme from epimastigote mitochondria by ion-exchange and gel filtration chromatography using the nonionic detergent sucrose monolaurate (Table 1). Decylubiquinone-mediated succinate: DCIP reductase activity was eluted as a single peak at each step

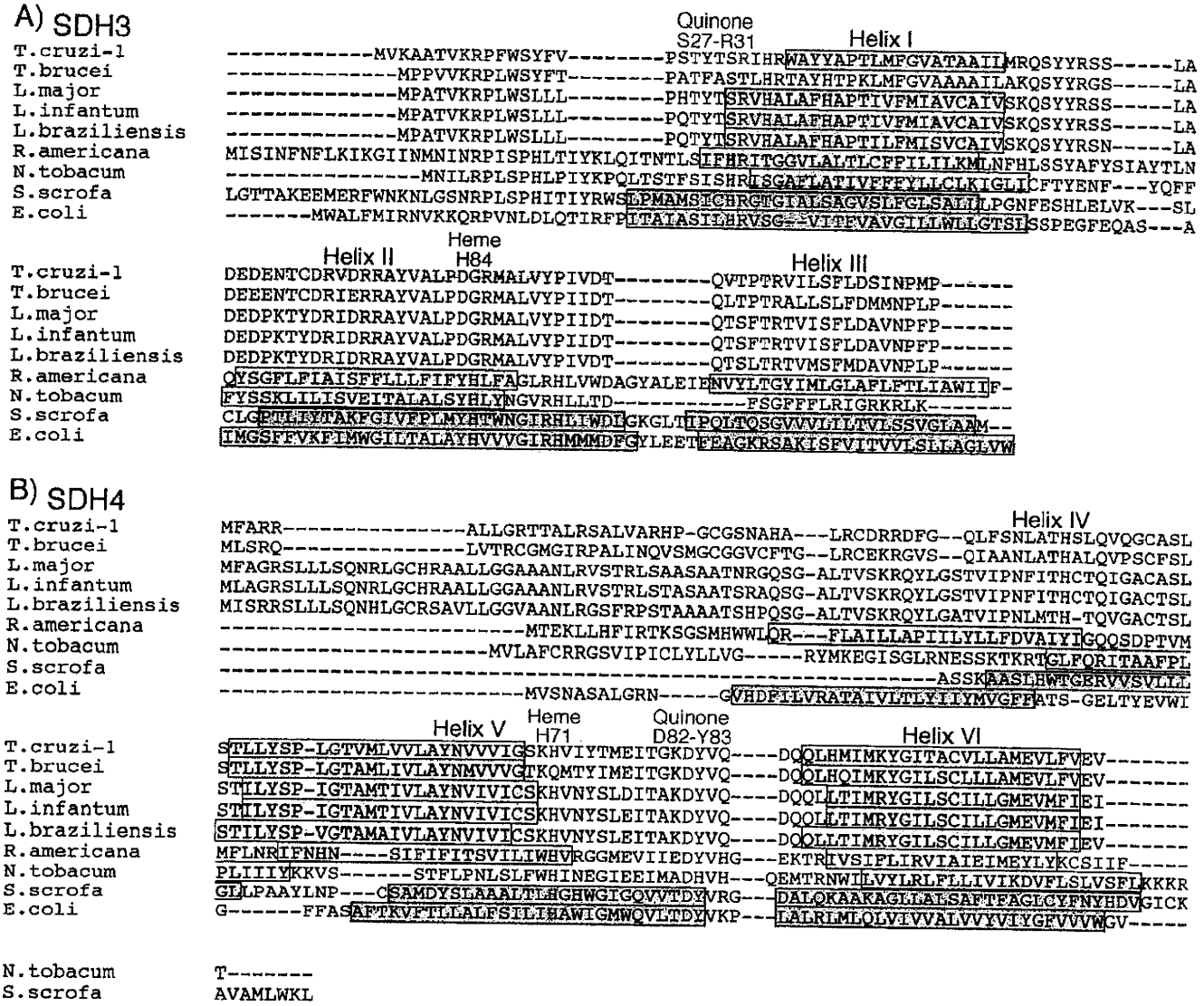

FIGURE 5. **Alignments of SDH3 (*A*) and SDH4 (*B*) sequences.** Amino acid residues proposed for binding of protoheme IX are shown in *red* and those for the quinone binding in *blue*. Other conserved residues are indicated by *green*. Transmembrane helices found in *E. coli* (Protein Data Bank code 1NEK) and porcine (Protein Data Bank code 1ZOY) Complex II are shown by *red rectangles*, and transmembrane helices predicted by TMHMM are indicated by *blue rectangles*. TMHMM failed to predict transmembrane helices in *T. brucei* SDH3. Residue numbers refer to *E. coli* SDH3 (SdhC) and SDH4 (SdhD). GenBank™ accession numbers for SDH3 and SDH4 sequences used are *T. cruzi* (XP_809410, XP_808211), *T. brucei* (XP_845531, XP_823384), *L. major* (XP_001684890, XP_001685874), *L. infantum* (XP_001467132), *L. brasiliensis* (XP_001566908, XP_001567905), *R. americana* (NP_044796, NP_044797), *Nicotiana tobacum* (YP_173376, YP_173457), *Sus scrofa* (1ZOY_C, 1ZOY_D), and *E. coli* (NP_415249, NP_415250).

and co-eluted with proteins and *b*-type cytochrome(s) at the second Superdex 200 chromatography (Fig. 2). Specific activity was increased 34-fold to 2.9 units/mg proteins, and the yield was ~2%. A hrCNE of the pure protein identified *T. cruzi* Complex II as an ~550-kDa complex (Fig. 3, *lanes 1* and *3*), which is 4-fold larger than bovine and yeast Complex II (130 kDa) and potato Complex II (150 kDa) (26, 27). Upon phase partitioning of the mitochondrial fraction with Triton X-114, the Complex II of *T. cruzi* was found only in the detergent-rich fraction (data not shown). Analysis of the detergent-rich fraction by hrCNE showed the Complex II as a single band at the same position as the pure enzyme (~550 kDa) (Fig. 3, *lanes 2* and *4*). These results indicated that the purified Complex II was obtained in its intact form. Interestingly, second dimensional analysis of both the purified Complex II and the detergent-rich fraction from phase partitioning with Triton X-114 with SDH activity showed that *T. cruzi* Complex II is composed of 12 subunits (Fig. 3, *lanes 5* and *6*). The same subunit composition was obtained by immunoaffinity purification of the partially purified enzyme (data not shown). The apparent molecular weight of the subunits ranges from 7.3 to 63 kDa (Fig. 3, *lanes 7* and *8*). Assuming the presence of equimolar amounts of subunits, a total molecular mass of Complex II would be 286.5 kDa, indicating that *T. cruzi* Complex II is a homodimer.

Identification of Genes Coded for Subunits—We determined N-terminal sequences (or internal peptide sequences in case of $SDH2_N$ and SDH8) of all subunits and identified genes coded for SDH1-1, $SDH2_N$, $SDH2_C$, SDH5–SDH7 (hydrophilic sub-